

## Control energy management system for photovoltaic with bidirectional converter using deep neural network

Widjonarko<sup>1</sup>, Wahyu Mulyo Utomo<sup>2</sup>, Saodah Omar<sup>3</sup>, Fatah Ridha Baskara<sup>1</sup>, Marwan Rosyadi<sup>4</sup>

<sup>1</sup>Department of Electrical Engineering, Faculty of Engineering, Universitas Jember, Jember, Indonesia

<sup>2</sup>Faculty of Electrical and Electronic Engineering, Universiti Tun Hussein Onn Malaysia, Batu Pahat, Malaysia

<sup>3</sup>Faculty of Electrical Engineering, Universiti Teknologi Mara Kampus Pulau Pinang, Pulau Pinang, Malaysia

<sup>4</sup>Department of Electrical Engineering, Faculty of Engineering, Universitas Muhammadiyah Surabaya, Surabaya, Indonesia

### Article Info

#### Article history:

Received May 22, 2023

Revised Sep 26, 2023

Accepted Nov 29, 2023

#### Keywords:

Energy storage

Extreme learning machine

Hybrid energy source system

Power management system

Renewable energy

### ABSTRACT

Rapid population growth propels technological advancement, heightening electricity demand. Obsolete fossil fuel-based power facilities necessitate alternative energy sources. Photovoltaic (PV) energy relies on weather conditions, posing challenges for constant energy consumption. This hybrid energy source system (HESS) prototype employs extreme learning machine (ELM) power management to oversee PV, fossil fuel, and battery sources. ELM optimally selects power sources, adapting to varying conditions. A bidirectional converter (BDC) efficiently manages battery charging, discharging, and secondary power distribution. HESS ensures continuous load supply and swift response for system reliability. The optimal HESS design incorporates a single renewable source (PV), conventional energy (PNL and genset), and energy storage (battery). Supported by a BDC with over 80% efficiency in buck and boost modes, it stabilizes voltage and supplies power through flawless ELM-free logic verification. Google Colab online testing and hardware implementation with Arduino demonstrate ELM's reliability, maintaining a direct current (DC) 24 V interface voltage and ensuring its applicability for optimal HESS.

This is an open access article under the [CC BY-SA](https://creativecommons.org/licenses/by-sa/4.0/) license.



### Corresponding Author:

Widjonarko

Department of Electrical Engineering, Faculty of Engineering, Universitas Jember

Kalimantan St., Number. 37 – Bumi Tegalboto Campus Mail box 159 Jember, East Java, 68121, Indonesia

Email: widjonarko.teknik@unej.ac.id

## 1. INTRODUCTION

The population explosion accelerates the present rate of technological advancement. The number of households is anticipated to reach 70.6 million by 2025 and approximately 80 million by 2050 [1]. Urbanization is expected to rise to 67% by 2035 [2], impacting energy requirements, particularly in the electricity sector. Electricity consumption is expected to increase from 60% in 2018 to 90% in 2050 [3]. The pervasive use of electronic household appliances is primarily responsible for rising energy demand [4]. Despite efforts to conserve electrical energy, such as inverters in air conditioning and energy-saving light bulbs, the electricity sector's use of fossil fuels has not decreased substantially [5]. Government policies and regulations have supported the development of renewable energy (RE), but the use of RE is still limited due to high production costs and technological and component limitations [6], [7].

Inconsistent energy availability is a primary obstacle to using RE [8]. The hybrid energy source system (HESS) concept has been developed To overcome this limitation [9]–[11]. HESS integrates multiple sources of electrical energy to meet load requirements [12]. Several methods, including energy storage, have been devised to incorporate energy sources [13]. For optimal efficacy, HESS calls for a reliable source and

load management system [14]. HESS requires an optimal control system to regulate its energy delivery strategy [14]. Control algorithms have been derived from mathematical control theory and artificial intelligence (AI) in several research investigations [15]–[17]. The majority of HESS-related research, however, is still in the simulation phase and has not been extensively implemented [18].

In previous research, HESS has been optimized using mathematical techniques such as active–reactive power (PQ) control and particle swarm optimization (PSO) [18]. Several studies have also employed artificial intelligent (AI)-based methods, including artificial neural networks (ANN). Management of HESS with AI has also been extensively studied, which uses deep reinforcement learning for microgrid applications [19], ANN for control management in base transceiver station (BTS) applications [13], and machine learning in energy dispatch applications in power systems [20]. In addition, Ferraro *et al.* [21] conducted research utilizing fuzzy logic control (FLC) as the control system, where wind energy is combined with energy storage to ensure uninterrupted operation of the uninterruptible power supply (UPS). Georgiou *et al.* [22] employ ANN as a method for load prediction with the combined algorithm system advisor model (SAM) for photovoltaic (PV) energy dispatch into the grid. Likewise, Vallem and Kumar [23] emphasizes the combination of energy sources. These studies use complex programming languages. In some cases, complex programming will cause failures in computing and cause decision-making errors when determining which source to use. This research implements a HESS simulation system with a control system using extreme learning machine (ELM) learning techniques. ELM was chosen because of its simple implementation, concise programming, fast iteration, and high performance [24], [25]. This research is intended to implement HESS in maintaining load supply continuity with effectiveness and quick response. So, the target is to be able to maintain a stable voltage of 24 V direct current (DC) and have continuity in supplying the power load.

## 2. METHOD

By using the ELM algorithm, this study employs a systematic research methodology to investigate and enhance power management in HESS. A thorough literature review on HESS, power management, and machine learning algorithms is the foundation for identifying research gaps and formulating specific research questions. The procedure for conducting research consists of several primary stages. First, a mathematical model and simulation of the HESS system, including multiple energy sources, energy storage, pressures, and control mechanisms, are developed. Next, the ELM algorithm is devised for the HESS system's power management. This entails defining input and output parameters, training the algorithm with suitable data sets, and optimizing performance. The ELM algorithm is then incorporated into the HESS system simulation, ensuring the algorithm's decision-making process, control strategies, and energy delivery mechanisms are well integrated.

The program is evaluated under a variety of operational conditions and energy consumption patterns. For simulation input, data collection includes energy generation, demand, and environmental variables. Energy efficiency, system stability, and response time are simulated using the ELM algorithm. These results are compared to benchmark scenarios or alternative control strategies to evaluate the algorithm. ELM affects the operation of the HESS system. Data is analyzed using statistical and computational approaches to assess the algorithm's performance in meeting research goals. Data are analyzed to improve HESS power management and outline future research. This study's design, methods, testing, and data collection are organized. Mathematical modelling, algorithm implementation, simulation, and data analysis can assess the enhancement of HESS's ELM algorithm's power management.

### 2.1. HESS block diagram

The proposed system layout is shown in Figure 1. A block diagram of a HESS system with a scenario of one renewable energy source (photovoltaic), conventional energy (PNL and genset), and energy storage (battery) using an Arduino Mega is used as a primary control. The Arduino Mega is the microcontroller that measures and selects the suitable energy sources for a load supply.

Arduino measures the voltage and current of all energy sources. The energy source selected by Arduino is based on the predefined binary criteria. The binary rules will be applied when the Arduino performs measurements on all ELM-trained sources. Arduino will be used to implement the ELM's Google Colab-programmed binary function and retrieve the Beta and weight parameters into the HESS system.

### 2.2. Bidirectional converter design

When considering the design of a bidirectional DC-DC converter (BDC) capable of both buck and boost operations, it is crucial to address two significant aspects: the high voltage side, also known as the DC bus, and the low voltage side, which pertains to the battery for charging and discharging purposes, precisely selecting three primary components, namely inductors, capacitors, and metal–oxide–semiconductor field-

effect transistors (MOSFETs). The best performance of both the buck and boost converters necessitates careful consideration of the selection of their respective components.

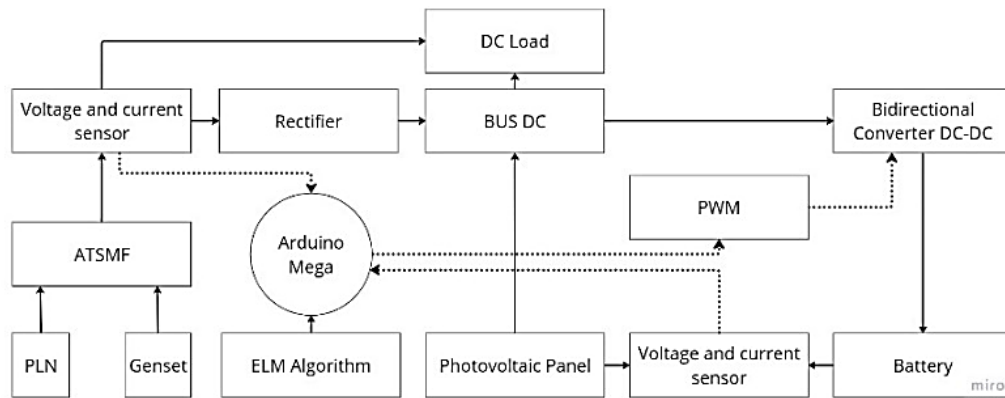


Figure 1. HESS control system design

### 2.2.1. Buck mode

The initial step in the process of inductor selection involves the determination of the duty cycle, which may be derived from (1).

$$D_1 = \frac{12}{24} \tag{1}$$

$$D_1 = 5 \tag{2}$$

In the design of converters, it is necessary to incorporate ripple. To optimize inductance, it is imperative to ensure little ripple is present in the design. In (3) has been cited and implemented in the proposed system, as indicated by the current research.

$$\Delta I = 0\% \times 4.2 \tag{3}$$

$$\Delta I = 0.42 \text{ ampere} \tag{4}$$

Subsequently, the minimum inductance value on the side of the buck converter can be calculated using (5).

$$L_{min} = \frac{24 \times 0.5 \times (1 - 0.5)}{20 \times 10^3 \times 0.42} \tag{5}$$

$$L_{min} = \frac{24 \times 0.25}{8400} \tag{6}$$

$$L_{min} = 714 \mu H \tag{7}$$

When utilizing an inductor, it is imperative to ensure that the chosen inductor has a minimum value of 714  $\mu F$ . After obtaining the duty cycle value, the initial stage in capacitor determination involves the determination of the voltage ripple value. Voltage ripple refers to the variation in voltage magnitude observed between the highest and lowest points in a waveform. The assumed value of 1% of the output voltage is incorporated into (8).

$$\Delta V = 1\% \times 24 \tag{8}$$

$$\Delta V = 0.24 \text{ volt} \tag{9}$$

Subsequently, one may determine the minimum capacitance value to be employed, as derived from (10).

$$C_1 = \frac{3}{0.24} \times 0.5 \times 16 \times 10^{-5} \tag{10}$$

$$C_1 = 12.5 \times 5 \times 10^{-5} \quad (11)$$

$$C_1 = 313 \mu F \quad (12)$$

Based on the obtained data, it is determined that the appropriate capacitance value for implementation on the buck converter side is 313  $\mu F$ .

### 2.2.2. Boost mode

Similar to the buck converter, determining the duty cycle value in (13) is also necessary for the boost side.

$$D_2 = \frac{24-12}{24} \quad (13)$$

$$D_2 = 0.5 \quad (14)$$

Furthermore, because the ripple current value has been expressed on the buck converter side and is deemed the same, the subsequent step involves determining the minimum inductor value of the boost converter, as derived from (15).

$$L_{min} = \frac{12 \times 0.5}{20 \times 10^3 \times 0.42} \quad (15)$$

$$L_{min} = \frac{6}{8400} \quad (16)$$

$$L_{min} = 714 \mu H \quad (17)$$

Based on the computation mentioned above, it can be asserted that the minimum inductance value of the boost converter is equivalent to that of the buck converter, amounting to 714  $\mu H$ . Implementing the inductor is important in BDC design, as it involves careful analysis and consideration. This study employed the T157-125 iron powder core, characterized by specific dimensions including an outside diameter of 39.9 mm, an inner diameter of 24.1 mm, and a height of 14.5 mm. Additionally, the core exhibited a permeability value of 125 and was paired with an enamel wire of 1 mm in diameter. To determine the number of windings, it is advisable to perform calculations based on the information provided in the preceding section,

$$\sqrt{\frac{714 \times 1.000}{(0.2 \times 125 \times 14.5 \times LN(\frac{39.9}{24.1}))}} \quad (18)$$

$$N = 62,504 \quad (19)$$

Based on the computed results, a total of 63 coils is necessary to attain the desired inductor value. The outcomes of the computations are applied directly to encase the central component with a copper layer measuring 1 mm in diameter in order to facilitate the passage of an electric current of roughly 5 amperes.

$$C_2 = 2.14 \times 313 \quad (20)$$

$$C_2 = 213.6 \mu F \quad (21)$$

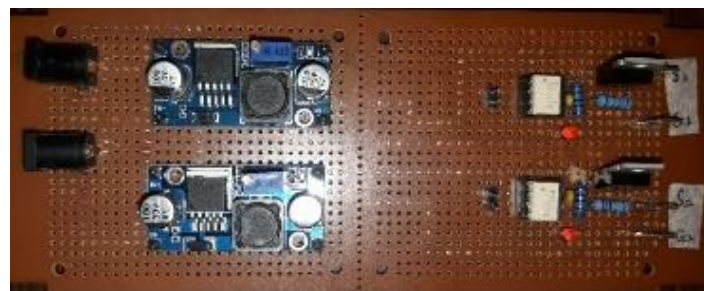
The subsequent step involves calculating the capacitance of the boost converter based on the reference value obtained from the buck converter, as expressed in (20). The selection of IRFP260 as the MOSFET for the switching operation conducted by the converter was made in this study. The specs of the IRFP260 MOSFET have previously been found to align with the requirements of the required system.

### 2.3. Bidirectional converter test

In this study, the bidirectional converter (BDC) driver testing methodology consists of three main stages. The initial step involves evaluating the pulse width modulation (PWM) driver circuit and adjusting the duty cycle based on the buck and boost calculations. These tests verify the PWM driver circuit can generate the correct duty cycle based on the previously calculated values. Testing the BDC algorithm for buck-boost operation is the second step. This testing determines if the algorithm performs as expected to

charge and sustain voltage stability during the energy discharge process. During this phase, the BDC algorithm is executed and monitored to ensure that it can perform effective charging and maintain voltage stability throughout the energy discharge process. Final testing of the BDC algorithm determines when the system should operate in buck mode and switch to boost mode under diverse conditions and loads. This testing is performed to evaluate the algorithm's ability to determine the proper mode based on the requirements of the system. During these tests, the essential testing conditions are created using equipment and instruments such as oscilloscopes, voltage and current meters, and load simulators. The test results will be used to evaluate the performance of the BDC algorithm, verify that the HESS system operated effectively, and optimize the use of buck and boost modes following the system's specifications.

As depicted in Figure 2(a), an optocoupler MOSFET driver with a switching frequency of 20 kHz is utilized in this investigation. Figure 2(b) illustrates that the bootstrap circuit consists of resistor and capacitor components to amplify the driver circuit and provide the required  $V_{gate}$ . Since the microcontroller's PWM voltage is limited to 5 V, it must be amplified using an auxiliary power supply. In this research, a 2-channel Hantek oscilloscope was used for experimental purposes. The strategic positioning of a buck-boost converter component holds significant importance within the framework of building a hybrid energy storage system (HESS). The utilization of BDC is employed for the purpose of regulating and optimizing the electrical current inside this particular system. Hence, when developing the BDC converter, it is imperative to meticulously consider the criteria outlined in the specified requirements. Initially, it is imperative for the bus output voltage generated by the BDC to attain a magnitude of 24 volts, while simultaneously ensuring that the bus output current achieves a value of 4.2 amperes. Furthermore, the voltage of the battery employed in this HESS is 12 volts. The recommended switching frequency for power switching by the BDC should be approximately 20 kHz. The system load is supplied with a voltage of 24 volts, while the load current is measured at 2.4 amperes.



(a)



(b)

Figure 2. Circuit components (a) BDC driver and (b) BDC implementation circuit

#### 2.4. Binary rules test

This study's binary rules testing methodology consists of two primary phases. Using Google Colab and Proteus applications, ELM rules are initially tested online. The ELM rules are directly executed through the Google Colab application during testing to evaluate the precision and efficacy of the generated rules. In addition, compatibility and system response are validated in a virtual simulation environment using the Proteus application. The second stage consists of offline testing of the Arduino principles using sensor reading scenarios. The system's ability to provide appropriate responses based on measured conditions is evaluated by inputting sensor data into Arduino and executing the rules offline. This testing uses an Arduino board, sensors, and Arduino programming applications to implement and manage the rules offline. Online

and offline testing results will be used to evaluate the performance and efficacy of the ELM rules for decision-making based on measured sensor data. In the context of binary rules, any variable can be categorized into two states: active and inactive, as shown in Table 1.

Table 1. HESS binary rules

Input				Output			
PV	BATT	PLN	GENSET	B <sub>CD</sub>	PLN	GENSET <sub>START</sub>	GENSET
0	0	0	0	0	0	0	0
0	0	0	1	0	0	1	1
0	0	1	0	0	1	1	0
0	0	1	1	0	1	0	0
0	1	0	0	1	0	0	0
0	1	0	1	1	0	0	0
0	1	1	0	1	0	0	0
0	1	1	1	1	0	0	0
1	0	0	0	0	0	0	0
1	0	0	1	0	0	0	0
1	0	1	0	0	0	0	0
1	0	1	1	0	0	0	0
1	1	0	0	1	0	0	0
1	1	0	1	1	0	0	0
1	1	1	0	1	0	0	0
1	1	1	1	1	0	0	0

### 3. RESULTS AND DISCUSSION

#### 3.1. Testing of the bidirectional converter

The purpose of the BDC testing was to ascertain the response of the duty cycle in PWM and the algorithm of the BDC used for battery charging and discharging. This testing was conducted to evaluate the BDC's efficacy. For observing the output waveform, a sample duty cycle of 50% was generated from Arduino Mega pins 11 and 12 for both buck and boost modes. The setting for voltage per division was 5 V. Figures 3(a) and 3(b) display the outcomes of the MOSFET driver testing.

As mentioned in Figure 3, the experimentation yielded two PWM signal waveforms. Figure 3(a) displays the buck-side PWM signal, whereas Figure 3(b) displays the boost-side PWM signal. The testing was divided into two sections. Starting with a state of charge (SOC) of 70%, the buck mode was tested with the BDC directly connected to the battery for charging. The second part involved evaluating the boost mode, in which various input voltage values were used to evaluate voltage regulation via discharge testing.

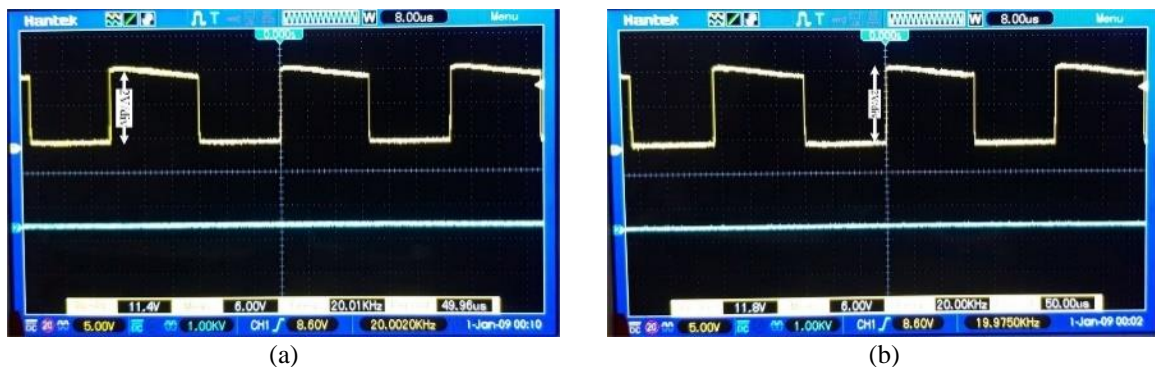


Figure 3. Results from testing of the MOSFET driver (a) buck mode and (b) boost mode

#### 3.1.1. Testing in the buck converter mode operation

From testing the buck mode on the BDC, the results are shown in Figure 4. This testing was performed to observe the data from BDC battery filling. The 70% was the initial SOC of the battery before testing. This test was conducted to verify that the BDC can charge the battery using the concept of constant voltage and constant current. The charging current is maintained at a constant value of 1 A, as depicted in Figure 4. During the charging procedure, as the battery's capacity increases, the voltage approaches 13.8 V. After reaching 13.8 V, the voltage remains constant at 14 V until the current reduces to 0.2 A or the capacity reaches 18 Ah.

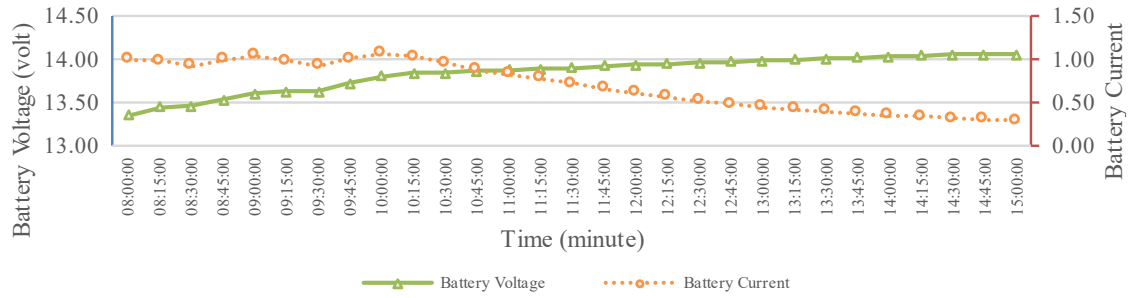


Figure 4. BDC buck mode testing for Kijo battery charging 12-volt 18 Ah

During the analysis of the buck mode testing in the BDC, a battery charging efficiency analysis of the converter was also performed. Table 2 displays the outcomes for a 12 V, 18-Ah Kijo battery. The input power was obtained from the power supply, which served as the battery power source at the time, and the output power was the power that the battery received. At 14.00 hours, the BDC obtained a 93% efficiency. Average efficiency during the charging procedure yields a result of 89%.

Table 2. BDC buck mode efficiency test results for Kijo battery charging 12-volt 18 Ah

Time (hours)	Power supply (watt)	Battery power (watt)	$\eta_{BDC}$ (%)
08:00:00	15.09	13.22	88%
09:00:00	15.92	14.21	89%
10:00:00	16.96	14.75	87%
11:00:00	13.08	11.45	88%
12:00:00	9.59	8.50	89%
13:00:00	7.00	6.26	89%
14:00:00	5.37	4.97	93%
15:00:00	4.45	4.04	91%
Average			89%

### 3.1.2. Testing in the boost converter mode operation

This aspect is tested to observe the line regulation and the stability of the output voltage on the bus voltage when the input voltage changes. The input voltage variations are simulated using a power supply to ascertain the influence of the line regulation in detail. The data collection results are depicted in Table 3.

The line regulation value is 5%, as indicated by the data presented in Table 2. This means that a 1 V increase or decrease on the low voltage side will result in a 5% change in the bus voltage. Given that the purpose of the boost side of the BDC is to maintain the stability of the bus DC voltage as the load supply using the battery, this is considered a positive result. In addition to deriving the line regulation value from these tests, the boost mode efficiency can also be determined, as shown in Table 4. From the test results of every 20 seconds, the BDC boost mode has an average efficiency of 83%. Analysis continues until the 40th second.

Table 3. Testing the boost side reviewing the BDC line regulation

Power supply voltage (volt)	Bus voltage (volt)	Bus current (ampere)	Line regulation (%)
10.43	21.04	0.16	5%
11.15	24.09	0.17	
12.06	24.19	0.16	
13.18	24.1	0.18	
14.12	24.05	0.17	

Table 4. BDC efficiency test results in boost mode

Time (second)	Bus power (watt)	Power of power supply (watt)	$\eta_{BDC}$ (%)
1	3.94	4.94	80%
20	3.97	4.92	81%
40	3.88	4.77	81%
60	3.92	4.68	84%
80	4.08	4.61	89%
Average			83%

**3.1.3. Algorithm testing two modes (buck and boost)**

This test was conducted to observe the configuration of the BDC with the load power, considering the PV-generated power using a power supply to simulate the PV-generated power. In this instance, the PV configuration is divided into three sections: first, affecting when the PV power is lower than the load power; second, simulating when the power is equal to the load power. In buck mode, the PV power exceeds the load power but is still sufficient to charge the load. Arduino instructs the PWM pin in boost mode to progressively increase its duty cycle to match the DC Bus voltage rating. In contrast, Arduino deactivates the buck mode MOSFET by setting the PWM value to 0. In the rest mode, all methods are inactive, so both MOSFETs' PWM values are 0. Figure 5 also briefly illustrates the power results from evaluating the BDC algorithm for the two modes.

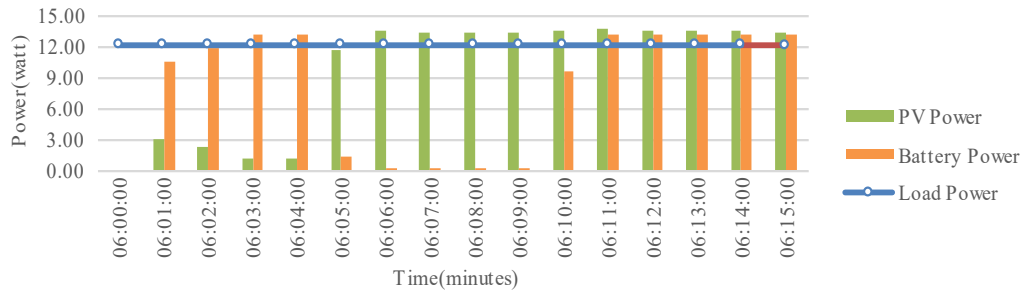


Figure 5. The relationship between supply power and load power in the BDC algorithm tester

**3.2. Testing of the ELM results on HESS**

Before implementing the ELM algorithm on the Arduino platform, it is necessary to make predictions using the entire dataset because the training data for regression patterns is different, and the data in the rules cannot be divided. In this instance, ELM obtains an accuracy value of 1, indicating that when testing online on the Google Colab platform, the rules produce 100 % accuracy (the provided accuracy range is between 0 and 1). The results of evaluating the effect of varying activation functions and the number of neurons on the level of precision are shown in Table 5.

The initial testing was conducted over 31 minutes to evaluate the output response of the provided rule scenarios. The results conformed to the rule design outlined. For instance, between minutes 10 and 13, the ELM response indicated the presence of signals from both the power grid (PLN) and the generator (genset) capable of supplying power to the load. Consequently, the output response at the time was to prioritize power supply through the power grid (PLN). From minute 20 to minute 22, the ELM indicated that the battery and power grid (PLN) contributed to the available power supply. As depicted in Figure 6, the battery was selected as the priority source to furnish the load in this instance. Other scenarios were also consistent with the predetermined objectives.

Figure 6 and Figure 7 illustrate the response of the DC bus voltage to the switching results of the power supply conducted by ELM. The DC bus voltage can fall within 24 V DC, although closer inspection reveals fluctuations within this range. This response indicates that through the system design of the HESS using ELM as the control for optimization, it is possible to obtain an optimal system while maintaining the DC bus value.

Table 5. ELM method test results for HESS on the Google Colab platform

No.	Activation function	Number of neurons	Waktu training (s)	Accuracy
1.	Rectified linear unit (ReLU)	10	0.00099	0.875
		100	0.00136	1
		1000	0.00385	1
2.	Sigmoid	10	0.00076	0.813
		100	0.00089	0.813
		1000	0.00275	0.813
3.	Tanh	10	0.00084	0.813
		100	0.00125	0.813
		1000	0.00813	0.813
4.	Softmax	10	0.00095	0.813
		100	0.00796	0.813
		1000	0.01005	0.813



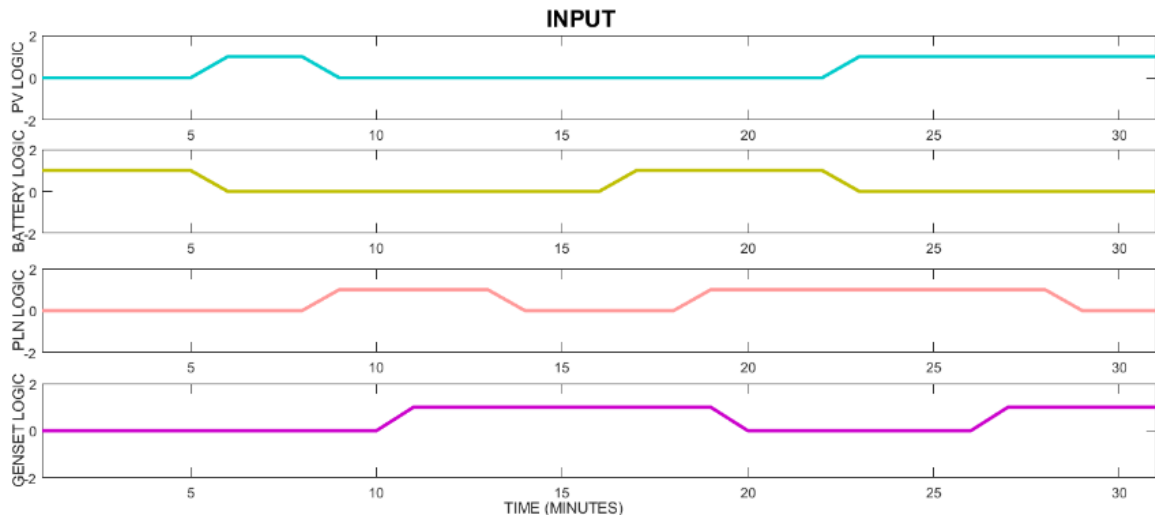


Figure 6. Input logic in HESS testing using ELM

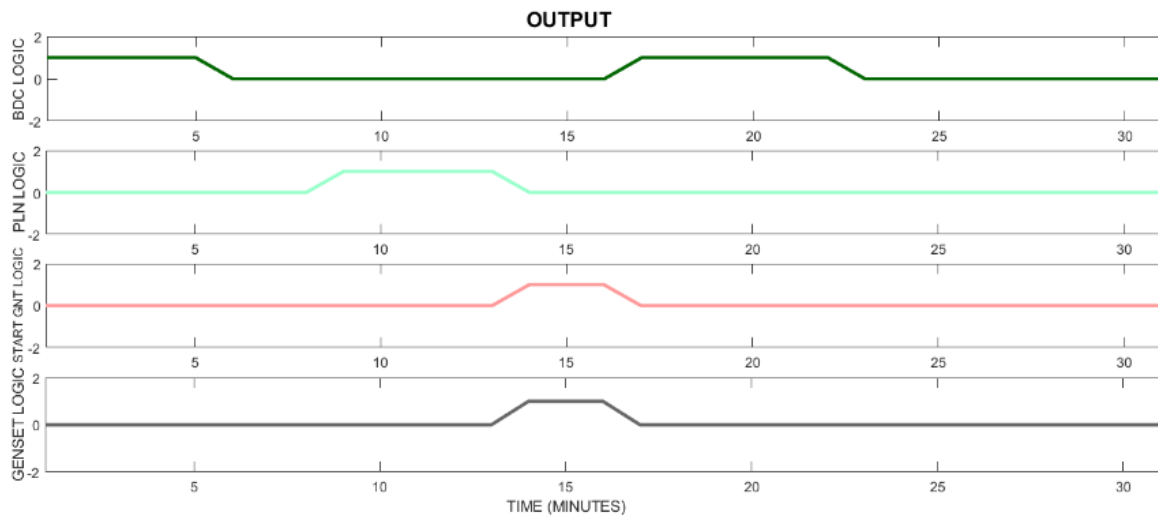


Figure 7. Output logic in HESS testing using ELM

#### 4. CONCLUSION

The ELM method has been successfully implemented, which has computational acceleration in creating optimal HESS using a BDC topology. The proposed method successfully maintains the stability and continuity of the load power supply against changes in the energy source provided. The proposed HESS configuration uses a BDC topology to supply load power, stabilize bus voltage and store excess capacity in the battery. From the efficiency testing results, the BDC has an efficiency above 80% in both modes, namely buck and boost. Then, in the proposed ELM method, HESS can run optimally without load power supply discontinuity occurring. The ELM method was tested online using Google Colab with training scenarios and code testing on the Google Colab platform, resulting in 100% accuracy. Meanwhile, for offline testing on the hardware (Arduino) section, HESS works optimally against changes in load power supply conditions with a logic 1 (active) output for the resulting load power supply and can maintain 24 V DC bus voltage. This is a breakthrough in the development of HESS technology, which requires reliability and accelerated decision-making in weather conditions with RE properties.

#### ACKNOWLEDGEMENTS




The author deeply thanks the University of Jember for their generous financial support.

## REFERENCES




- [1] UN, "Population 2030: demographic challenges and opportunities for sustainable development planning (ST/ESA/SER.A/389)," *United Nations*, pp. 1-58, 2015.
- [2] F. H. Mardiansjah, P. Rahayu, and D. Rukmana, "New patterns of urbanization in Indonesia: emergence of non-statutory towns and new extended urban regions," *Environment and Urbanization ASIA*, vol. 12, no. 1, pp. 11–26, 2021, doi: 10.1177/0975425321990384.
- [3] M. Larsson, *Global energy transformation*. London: Palgrave Macmillan UK, 2009.
- [4] M. González-Torres, L. Pérez-Lombard, J. F. Coronel, I. R. Maestre, and D. Yan, "A review on buildings energy information: trends, end-uses, fuels and drivers," *Energy Reports*, vol. 8, pp. 626–637, Nov. 2022, doi: 10.1016/j.egy.2021.11.280.
- [5] K. Harby and F. Al-Amri, "An investigation on energy savings of a split air-conditioning using different commercial cooling pad thicknesses and climatic conditions," *Energy*, vol. 182, pp. 321–336, 2019, doi: 10.1016/j.energy.2019.06.031.
- [6] Seetharaman, K. Moorthy, N. Patwa, Saravanan, and Y. Gupta, "Breaking barriers in deployment of renewable energy," *Heliyon*, vol. 5, no. 1, 2019, doi: 10.1016/j.heliyon.2019.e01166.
- [7] IESR, "Indonesia energy transition outlook 2022. Tracking progress of energy transition in Indonesia: aiming for Net-Zero emissions by 2050," Institute for Essential Services Reform (IESR), Jakarta, 2021.
- [8] D. Gielen, F. Boshell, D. Saygin, M. D. Bazilian, N. Wagner, and R. Gorini, "The role of renewable energy in the global energy transformation," *Energy Strategy Reviews*, vol. 24, pp. 38–50, 2019, doi: 10.1016/j.esr.2019.01.006.
- [9] W. Jing, C. H. Lai, S. H. W. Wong, and M. L. D. Wong, "Battery-supercapacitor hybrid energy storage system in standalone DC microgrids: A review," *IET Renewable Power Generation*, vol. 11, no. 4, pp. 461–469, 2017, doi: 10.1049/iet-rpg.2016.0500.
- [10] I. E. Atawi, A. Q. Al-Shetwi, A. M. Magableh, and O. H. Albalawi, "Recent advances in hybrid energy storage system integrated renewable power generation: configuration, control, applications, and future direction," *Batteries*, vol. 9, no. 1, 2023, doi: 10.3390/batteries9010029.
- [11] A. Palatel, "Isolated hybrid energy systems for remote locations," *Encyclopedia of Sustainable Technologies*, pp. 205–216, 2017, doi: 10.1016/B978-0-12-409548-9.10145-9.
- [12] X. Lin and R. Zamora, "Controls of hybrid energy storage systems in microgrids: critical review, case study and future trends," *Journal of Energy Storage*, vol. 47, 2022, doi: 10.1016/j.est.2021.103884.
- [13] Widjonarko, C. Avian, S. B. Utomo, A. Setiawan, and B. Rudiyanto, "A control strategy for hybrid energy source in backbone base transceiver station using artificial neural network: a case study of Penajam, Indonesia," *International Journal of Energy and Environmental Engineering*, vol. 11, no. 4, pp. 405–416, 2020, doi: 10.1007/s40095-020-00348-y.
- [14] A. Aktas, K. Erhan, S. Ozdemir, and E. Ozdemir, "Experimental investigation of a new smart energy management algorithm for a hybrid energy storage system in smart grid applications," *Electric Power Systems Research*, vol. 144, pp. 185–196, 2017, doi: 10.1016/j.epsr.2016.11.022.
- [15] I. H. Sarker, "AI-based modeling: techniques, applications and research issues towards automation, intelligent and smart systems," *SN Computer Science*, vol. 3, no. 2, Mar. 2022, doi: 10.1007/s42979-022-01043-x.
- [16] R. I. Mukhamediev *et al.*, "Review of artificial intelligence and machine learning technologies: classification, restrictions, opportunities and challenges," *Mathematics*, vol. 10, no. 15, 2022, doi: 10.3390/math10152552.
- [17] Y. Xu *et al.*, "Artificial intelligence: a powerful paradigm for scientific research," *Innovation*, vol. 2, no. 4, 2021, doi: 10.1016/j.xinn.2021.100179.
- [18] M. Arslan, I. Ahmad, M. K. Azeem, and M. Liaquat, "Dual-stage adaptive control of hybrid energy storage system for electric vehicle application," *Journal of Energy Storage*, vol. 43, 2021, doi: 10.1016/j.est.2021.103165.
- [19] L. Lei, Y. Tan, G. Dahlenburg, W. Xiang, and K. Zheng, "Dynamic energy dispatch based on deep reinforcement learning in IoT-driven smart isolated microgrids," *IEEE Internet of Things Journal*, vol. 8, no. 10, pp. 7938–7953, 2021, doi: 10.1109/JIOT.2020.3042007.
- [20] L. Yin *et al.*, "A review of machine learning for new generation smart dispatch in power systems," *Engineering Applications of Artificial Intelligence*, vol. 88, 2020, doi: 10.1016/j.engappai.2019.103372.
- [21] M. Ferraro, G. Brunaccini, F. Sergi, D. Aloisio, N. Randazzo, and V. Antonucci, "From uninterruptible power supply to resilient smart micro grid: the case of a battery storage at telecommunication station," *Journal of Energy Storage*, vol. 28, 2020, doi: 10.1016/j.est.2020.101207.
- [22] G. S. Georgiou, P. Nikolaidis, S. A. Kalogirou, and P. Christodoulides, "A hybrid optimization approach for autonomy enhancement of nearly-zero-energy buildings based on battery performance and artificial neural networks," *Energies*, vol. 13, no. 14, 2020, doi: 10.3390/en13143680.
- [23] V. V. S. N. M. Vallem and A. Kumar, "Optimal energy dispatch in microgrids with renewable energy sources and demand response," *International Transactions on Electrical Energy Systems*, vol. 30, no. 5, May 2020, doi: 10.1002/2050-7038.12328.
- [24] J. Wang, S. Lu, S. H. Wang, and Y. D. Zhang, "A review on extreme learning machine," *Multimedia Tools and Applications*, vol. 81, no. 29, pp. 41611–41660, 2022, doi: 10.1007/s11042-021-11007-7.
- [25] K. Zhang and M. Luo, "Outlier-robust extreme learning machine for regression problems," *Neurocomputing*, vol. 151, no. P3, pp. 1519–1527, 2015, doi: 10.1016/j.neucom.2014.09.022.

## BIOGRAPHIES OF AUTHORS






**Widjonarko**    receive Dr (Doctor) degree in electrical engineering from Brawijaya University, Malang, in 2019. He serves as Director of Undergraduate Studies in Electrical Engineering and Head of the research group on Automation and Technology in Industry. His research interests are energy, electrical engineering, control systems, power electronics, and applied electronics. He has published over ten papers in national journals and 12 international journals. He can be contacted at email: widjonarko.teknik@unej.ac.id.






**Wahyu Mulyo Utomo**    specializes in power electronics, electric motor actuators, and online neural networks. Universiti Teknologi Malaysia awarded him a Ph.D. in electrical engineering, Institut Teknologi Sepuluh Nopember an M.Eng., and Universitas Brawijaya a B.Eng. Dr. Utomo teaches at Universiti Tun Hussein Onn Malaysia since 2008. His expertise in power electronics, electric motor drives, and online neural networks is well-known. Dr. Utomo improves power electronic systems, particularly electric motor drives. He also studies power electronic system optimization using online neural networks. Publications in prestigious international journals have enhanced his competence. He can be contacted at email: wahyu@uthm.edu.my.






**Saodah Omar**    is an author from Universiti Teknologi MARA. Dr. Omar earned a power electronics-focused doctorate. Dr. Omar studies power electronics in smart grids. Dr. Omar uses power electronics and smart grid technology to improve power distribution and management. Dr. Saodah Omar is a prolific author, has advanced power electronics research. Their study illuminates smart grid technologies and power electronics. Dr. Omar's power electronics knowledge and Universiti Teknologi MARA affiliation make them an invaluable academic resource. Dr. Omar's research and dedication advance power electronics and smart grid technologies. He can be contacted at email: saodah004@uitm.edu.my.



**Fatah Ridha Baskara**    is an author that get bachelor degree in Electrical Engineering Department at Universitas Jember, Jember, Indonesia. He became an assistant laboratory in Electrical Energy Conversion Laboratory. His current research interests include power electronics and their applications, renewable energy and PCB design. He can be contacted at email: fatah.ridha99@gmail.com.



**Marwan Rosyadi**    obtained his Bachelor of Science degree (equivalent to *Sarjana Teknik*) in electrical engineering from Adhi Tama Institute of Technology Surabaya in 2004. He then pursued his Master of Engineering degree in electrical engineering from Sepuluh Nopember Institute of Technology, Indonesia, in 2006. Currently, he is actively pursuing his Ph.D. degree at Kitami Institute of Technology, Kitami, Hokkaido, Japan. Marwan Rosyadi serves as the Head of R&D for the Renewable Energy Unit at PT. Indah Karya (Persero). Additionally, he holds the position of research fellow at the Laboratory of Electric Machinery within the Department of Electrical and Electronic Engineering at Kitami Institute of Technology. He can be contacted at email: rosyadi@um-surabaya.ac.id.